Hindered Internal Conversion in Rigid Media. Thermally Nonequilibrated ^{3}IL and ^{3}CT Emissions from $[Cu(5\text{-}X\text{-}phen)(PPh_3)_2]^+$ and $[Cu(4,7\text{-}X_2\text{-}phen)(PPh_3)_2]^+$ Systems in a Glass at 77 K

Dominick J. Casadonte, Jr., and David R. McMillin*

Contribution from the Department of Chemistry, Purdue University, West Lafayette, Indiana 47907. *Received July 17, 1986*

Abstract: The photophysical properties of two series of mixed-ligand copper(I) complexes involving substituted 1,10-phenanthroline (phen) derivatives have been investigated in low-temperature glasses. In particular, the absorption and emission spectra of complexes of the type $[Cu(5\text{-}X\text{-}phen)(PPh_3)_2]^+$ or $[Cu(4,7\text{-}X_2\text{-}phen)(PPh_3)_2]^+$ have been characterized. The emission spectra are noteworthy because separate, nonequilibrated emissions are observed from two triplet excited states with distinct orbital parentages. The vibronically structured component of the emission has a lifetime of the order of 10 ms and has been assigned to a ^{3}IL (intraligand) excited state, while the broad, unstructured component, which has a lifetime of the order of 100 μs, has been attributed to a ^{3}CT (charge-transfer) excited state. Although microenvironmental heterogeneity exists within the sample, it is argued that separate emissions occur because there is a structurally imposed barrier against interconversion between the ^{3}IL and ^{3}CT states in a rigid matrix. The relative energies of the ^{3}CT and ^{3}IL excited states vary, but the maximum energy difference between the zero-zero energies of the two states is about 1000 cm^{-1}. In all cases the emission from the lower energy component is more intense, and the relative intensity of the higher energy component decreases as the separation between states increases. Internal conversion beteen the two triplet states is viewed as an intramolecular electron-transfer process whose rate depends upon the driving force.

On the basis of studies of the luminescent properties of aromatic molecules, Kasha formulated his famous rule which states that for any given multiplicity only the lowest energy excited state is emissive.[1] For transition metal complexes intersystem crossing between excited states is usually an extremely facile process; hence one might anticipate that only *the* lowest energy excited state is apt to be emissive. However, several different types of excited states occur in these systems including metal-centered (MC), intraligand (IL), and charge-transfer (CT) excited states, and they are often closely spaced in energy. Thus, emission is observed from not only the lowest energy state but any others which can be thermally populated.[2] More recently, it has become clear that one may observe emissions from proximate excited states even when they are not thermally equilibrated, especially in rigid media at low temperatures.[3]

Dynamic processes connecting proximate excited states are of fundamental importance in the photophysics and photochemistry of transition metal complexes. For example, population of an upper excited state with a favorable radiative rate increases the emission quantum yield.[4] Alternatively, thermally accessible states which undergo efficient nonradiative decay and/or photochemistry may decrease the emission yield and even dictate the excited-state reactivity.[5-8] Finally, such systems may provide means for the detection of thermal energy by optical methods.[9]

Neighboring excited states may be distinguished by spin multiplicity,[4,10-15] the spin-orbit interaction,[16] spatial localization of the excitation,[17-20] or electronic configuration.[3,9,14,21-29] Although multiple emissions have been observed from proximate

Table I. Microanalytical Data

X	Y	% C calcd	% C anal.	% H calcd	% H anal.
		$[Cu(5\text{-}X\text{-}phen)(PPh_3)_2]Y$			
H	BF_4^-	67.60	67.34	4.37	4.67
CH_3	BF_4^-	67.71	67.34	4.37	4.78
Cl	BF_4^-	64.81	64.73	4.52	4.30
Ph	BF_4^-	69.65	69.15	4.55	4.89
		$[Cu(4,7\text{-}X_2\text{-}phen)(PPh_3)_2]Y$			
H	BF_4^-	67.60	67.34	4.37	4.67
Cl	BF_4^-	62.39	62.85	3.93	4.99
CH_3	$SO_3CF_3^-$	64.79	64.20	4.48	4.36
Ph	$SO_3CF_3^-$	68.50	68.27	4.33	4.21

(1) Kasha, M. *Discuss. Faraday Soc.* **1950**, *9*, 14-19.
(2) See, for example: Demas, J. N.; Crosby, G. A. *J. Am. Chem. Soc.* **1970**, *92*, 7262-7270.
(3) For a review of the literature which appeared up to about 1980, see: DeArmond, M. K.; Carlin, C. M. *Coord. Chem. Rev.* **1981**, *36*, 325-355.
(4) Kirchhoff, J. R.; Gamache, R. E., Jr.; Blaskie, M. W.; Del Paggio, A. A.; Lengel, R. K.; McMillin, D. R. *Inorg. Chem.* **1983**, *22*, 2380-2384.
(5) Van Houten, J.; Watts, R. J. *Inorg. Chem.* **1978**, *17*, 3381-3385.
(6) Durham, B.; Caspar, J. V.; Nagle, J. K.; Meyer, T. J. *J. Am. Chem. Soc.* **1982**, *104*, 4803-4810.
(7) Wacholtz, W. M.; Auerbach, R. A.; Schmehl, R. H.; Ollino, M.; Cherry, W. R. *Inorg. Chem.* **1985**, *24*, 1758-1760.
(8) Kirchhoff, J. R.; McMillin, D. R.; Marnot, P. A.; Sauvage, J. P. *J. Am. Chem. Soc.* **1985**, *107*, 1138-1141.
(9) Highland, R. G.; Crosby, G. A. *Chem. Phys. Lett.* **1985**, *119*, 454-458.
(10) Blasse, G.; McMillin, D. R. *Chem. Phys. Lett.* **1980**, *70*, 1-3.
(11) Gouterman, M.; Mathies, R. A.; Smith, B. E.; Caughey, W. S. *J. Chem. Phys.* **1970**, *52*, 3795-3802.
(12) Miskowski, V. M.; Nobinger, G. L.; Kliger, D. S.; Hammond, G. S.; Lewis, N. S.; Mann, K. R.; Gray, H. B. *J. Am. Chem. Soc.* **1978**, *100*, 485-488.
(13) Kenney, M. I. S.; Kenney, J. W., III, Crosby, G. A. *Organometallics* **1986**, *5*, 230-234.
(14) Castelli, F.; Forster, L. S. *J. Am. Chem. Soc.* **1975**, *97*, 6306-6309.
(15) Sexton, D. A.; Ford, P. C.; Magde, D. *J. Phys. Chem.* **1983**, *87*, 197-199.
(16) Brummer, J. G.; Crosby, G. A. *Inorg. Chem.* **1985**, *24*, 552-558.
(17) Halper, W.; DeArmond, M. K. *J. Lumin.* **1972**, *5*, 225-237.
(18) Watts, R. J.; Van Houten, J. *J. Am. Chem. Soc.* **1978**, *100*, 1718-1721.
(19) Kober, E. M.; Sullivan, B. P.; Meyer, T. J. *Inorg. Chem.* **1984**, *23*, 2098-2104.
(20) Braterman, P. S.; Heath, G. A.; Yellowlees, L. J. *J. Chem. Soc., Dalton Trans.* **1985**, *1081*-1085.
(21) Nishizawa, M.; Suzuki, T. M.; Sprouse, S.; Watts, R. J.; Ford, P. C. *Inorg. Chem.* **1984**, *23*, 1837-1841.
(22) Fredericks, S. M.; Luong, J. C.; Wrighton, M. S. *J. Am. Chem. Soc.* **1979**, *101*, 7415-7417.
(23) Buckner, M. T.; Matthews, T. G.; Lytle, F. E.; McMillin, D. R. *J. Am. Chem. Soc.* **1979**, *101*, 5846-5848.
(24) Radjaipour, M.; Oelkrug, D. *Ber. Bunsenges. Phys. Chem.* **1978**, *82*, 159-163.
(25) Rader, R. A.; McMillin, D. R.; Buckner, M. T.; Matthews, T. G.; Casadonte, D. J.; Lengel, R. K.; Whittaker, S. B.; Darmon, L. M.; Lytle, F. E. *J. Am. Chem. Soc.* **1981**, *103*, 5906-5912.
(26) Seegers, D. P.; DeArmond, M. K.; Grutsch, P. A.; Kutal, C. *Inorg. Chem.* **1984**, *23*, 2874-2878.

0002-7863/87/1509-0331$01.50/0

levels of a number of transition metal systems, few systematic investigations of the excited-state dynamics have been carried out. To this end we have been investigating complexes of the type $[Cu(NN)(PPh_3)_2]^+$ where NN denotes a derivative of 1,10-phenanthroline (phen). Previously, we showed that $[Cu(phen)(PPh_3)_2]^+$ and $[Cu(dmp)(PPh_3)_2]^+$, where dmp denotes 2,9-dimethyl-1,10-phenanthroline, exhibit ^{3}IL and ^{3}CT emissions in rigid, low-temperature glasses.[23,25] In order to carry out more detailed analyses, we have now investigated a number of complexes in which the phen ligand carries substituents at the 5 or the 4,7 positions, thus avoiding steric complications which occur with substituting the 2,9 positions.[30] The results show that there is a significant barrier to interconversion between the ^{3}IL and ^{3}CT excited states in rigid, low-temperature media and that the intervening energy gap is a key factor determining the relative intensities and the lifetimes of the emission components.

Experimental Section

Materials. The mixed-ligand complexes were synthesized by a previously reported method[25] and were recrystallized from ethanol. Microanalytical data are provided in Table I. The phenanthroline ligands were purchased from G. F. Smith Chemical Co., except for 4,7-dichloro-1,10-phenanthroline, which was a gift from C. P. Kubiak of Purdue University. All phenanthroline ligands were used without further purification. Triphenylphosphine (PPh_3) was obtained from Aldrich Chemical Co. and recrystallized twice prior to use. The source of copper was $Cu(O_3SCF_3)_2 \cdot xH_2O$ or $Cu(BF_4)_2 \cdot xH_2O$ which was prepared by the reaction of $Cu_2(OH)_2CO_3 \cdot H_2O$ with the appropriate strong acid.

All solvents were of the highest available purity. Ethanol was obtained from U.S. Industrial Chemicals Co., and methanol was from Burdick and Jackson ("Distilled in Glass" grade). Methylene chloride and chloroform were "photorex" grade from Baker Chemical Co.

Instrumentation. Absorption spectra were measured with a Cary 17D or an IBM Instruments Inc. Model 9430 UV-visible spectrophotometer. Steady-state emission spectra were measured with a Perkin-Elmer MPF-44B fluorescence spectrophotometer. The analogue output was sent to an Apple IIE microcomputer by way of a Cyborg Corp. Isaac 91A interface. Data acquisition and manipulation were accomplished with a user-written software package. Hard copies were recorded on a Hewlett-Packard Model 7470A serial plotter. Long-lived components (half-life > 1 ms) were obtained by viewing the emission through a user-built, rotating-can phosphoroscope which could be introduced into the sample compartment of the fluorescence instrument.

Pulsed-laser excitation was achieved with an EG&G Model 2100 Dyescan (nitrogen-pumped) dye laser. The luminescence signal was monitored with a phototube (either a Hamamatsu 746, an RCA 4840, or an RCA 931A) powered by a Pacific Instruments Model 227 power supply and hard-wired for fast response.[31] Variable-wavelength sampling was achieved with an Instruments SA Inc. H10 stepper-driven monochromator. The photocurrent was sent either to a Tektronix Inc. Model 465B oscilloscope, where it was photographed with a Tektronix C-5C camera, or to an EG&G Model 162 boxcar averager with a Model 165 gated integrator. In turn, the boxcar output was directed either to the Isaac/Apple IIE data facility or to a Hewlett-Packard Model 7015B X-Y recorder.

Low-temperature measurements were obtained with the aid of a quartz finger dewar or an Oxford Instruments Model DN704 cryostat. For the latter, temperature control was achieved with a controller which was custom-designed and constructed by G. W. Kramer of Purdue University.

Methods. All low-temperature measurements with the fluorometer were obtained in the dc operation mode to avoid suppression of the millisecond components. Room-temperature samples and all samples measured in the cryostat were subjected to a series of freeze–pump–thaw cycles to remove oxygen. The samples used in the finger dewar were simply frozen in liquid nitrogen as diffusion of O_2 was negligible in the glass state. For the time-resolved spectra measured with the boxcar averager a 5-ns gate was used, and the signal was sampled ca. 1 μs after the laser pulse. All lifetimes were calculated from standard log plots.

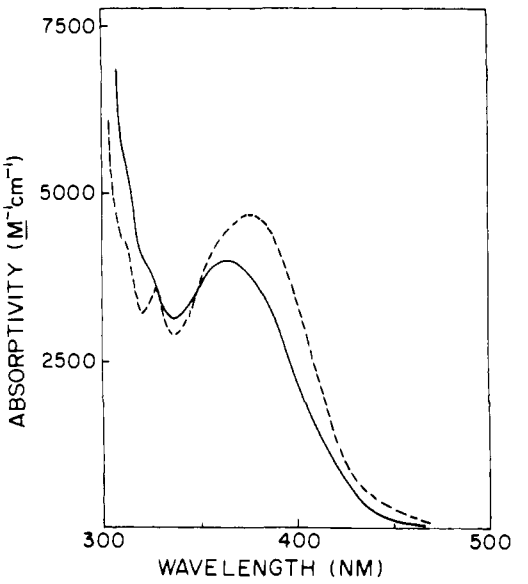

Figure 1. Absorption spectrum of $[Cu(phen)(PPh_3)_2]^+$ at 298 K (—) and 77 K (---). For the latter relative absorbance values are indicated.

Table II. Absorption Maxima in 4:1 EtOH/MeOH

X	300 K λ_{max}, nm	300 K ϵ, M^{-1} cm^{-1}	77 K λ_{max}, nm
	$[Cu(5\text{-}X\text{-}phen)(PPh_3)_2]^+$		
H	365	4000	378
	325 (sh)		329
			312 (sh)
CH_3	368	3500	381
			325
			318
Cl	374	3700	385
	330 (sh)		324
			319 (sh)
Ph	372	4300	383
			335 (sh)
	$[Cu(4,7\text{-}X_2\text{-}phen)(PPh_3)_2]^+$		
H	365	4000	378
	325 (sh)		329
			312 (sh)
Cl	386	2700	392
	332 (sh)		338
			320
CH_3	363	4300	372
			325
			310 (sh)
Ph	375	4700	385
			313 (sh)

The lifetimes of the millisecond components were measured by a variation of the method of Lewis and Kasha[32] with a 1-MΩ terminator on the oscilloscope, while a 10-kΩ terminator was used for the submillisecond lifetimes.

Results

Absorption Measurements. Each complex exhibits broad, structureless absorption in the near-UV region with an absorption maximum in the range of 360–390 nm, absorption which has previously been assigned as a metal-to-ligand charge-transfer (CT) transition.[25] As a representative case, the absorption spectrum of $[Cu(phen)(PPh_3)_2]^+$ in 4:1 EtOH/MeOH (v/v) is presented in Figure 1 in fluid solution (300 K) and in a low-temperature glass (77 K). Above the CT absorption, before the onset of the intense intraligand absorption, one or more somewhat narrower absorption bands are also resolved (Figure 1). These transitions can be assigned to IL absorption of the phenanthroline ligands as analogous bands are observed in the spectra of the uncoordi-

(27) Manuta, D. M.; Lees, A. J. *Inorg. Chem.* **1983**, *22*, 572–573.
(28) Merrill, J. T.; DeArmond, M. K. *J. Am. Chem. Soc.* **1979**, *101*, 2045–2055.
(29) Servaas, P. C.; van Dijk, H. K.; Snoeck, T. L.; Stufkens, D. J.; Oskam, A. *Inorg. Chem.* **1985**, *24*, 4494–4498.
(30) Kirchhoff, J. R.; McMillin, D. R.; Robinson, W. R.; Powell, D. R.; McKenzie, A. T.; Chen, S. *Inorg. Chem.* **1985**, *24*, 3928–3933.
(31) Harris, J. M.; Lytle, F. E.; McCain, T. C. *Anal. Chem.* **1976**, *48*, 2095–2098.
(32) Lewis, G. N.; Kasha, M. *J. Am. Chem. Soc.* **1944**, *66*, 2100–2116.

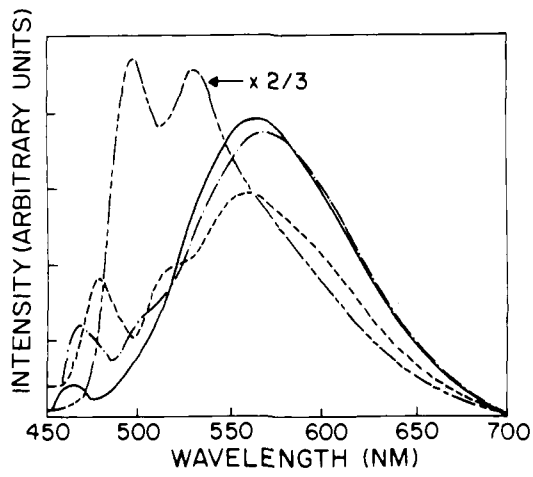

Figure 2. Uncorrected emission spectra of $[Cu(5\text{-X-phen})(PPh_3)_2]^+$ at 77 K: X = H (—); X = CH_3 (---); X = Cl (---); X = Ph (----). Excitation and emission slits were set at 8 nm, and the excitation wavelength was 380 nm.

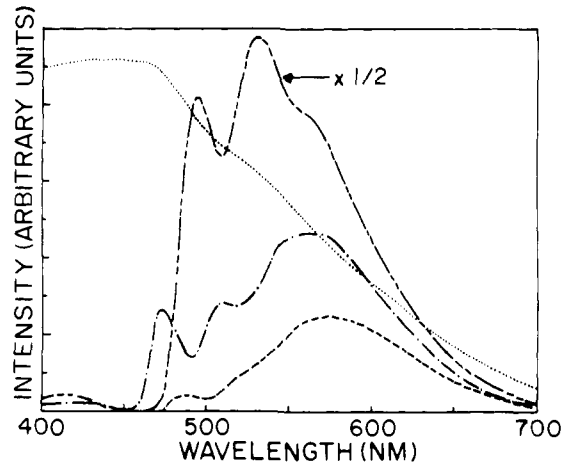

Figure 3. Uncorrected emission spectra of $[Cu(4,7\text{-}X_2\text{-phen})(PPh_3)_2]^+$: X = CH_3 (---); X = Cl (---); X = Ph (----); instrumental response (···). The excitation wavelength was 380 nm, and the emission and the excitation slits were set at 5 nm.

nated ligands. The same transitions also occur in the near-UV absorption spectrum of $[Ag(phen)(PPh_3)_2]^+$.[33] Relevant band maxima are listed in Table II.

The broad CT absorption band characteristic of $[Cu(phen)(PPh_3)_2]^+$ bleaches over a period of days or weeks when a solution stands in the presence of oxygen. If sodium ascorbate is added to the bleached solution, a broad absorption band develops with a maximum near 435 nm, attributable to $[Cu(phen)_2]^+$.[33] These results reveal that the complex is slowly autooxidized in solution, and that the phosphine ligands are modified at some point—presumably by conversion to the phosphine oxide. However, the reaction is quite slow. In order to avoid working with oxidized samples, freshly prepared solutions were used in all of our photophysical studies.

Low-Temperature Luminescence. Although the mixed-ligand complexes exhibit extremely weak photoluminescence in a 4:1 EtOH/MeOH solvent at room temperature, the emission is quite strong in the vitreous state at 77 K. Total emission spectra are presented in Figures 2 and 3 and the various emission maxima are compiled in Table III. The emission envelopes resemble the absorption spectra in that each complex exhibits a series of relatively sharp emission bands which merge into the high-energy side of a broad, structureless component. As discussed below, the unstructured component originates from a ^3CT excited state while the vibronically structured emission originates from a ^3IL excited state. The relative intensities of the ^3CT and ^3IL emissions are unaffected by the presence of excess phosphine but do vary with solvent composition. The total emission spectrum of $[Cu(5\text{-Cl-phen})(PPh_3)_2]^+$ is depicted in three different solvents in Figure 4, where excitation was at the CT absorption maximum in each case.

(33) Casadonte, D. J.; McMillin, D. R., unpublished results.

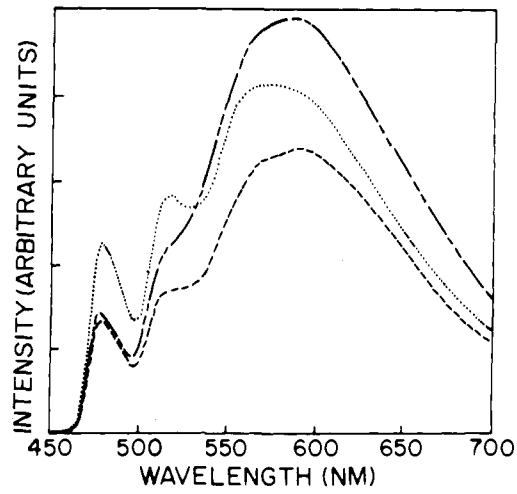

Figure 4. Solvent dependence of $[Cu(5\text{-Cl-phen})(PPh_3)_2]^+$ emission at 77 K: (----) EtOH/MeOH; (---) CH_2Cl_2; (···) $CHCl_3$. The excitation slit was set at 8 nm, and the emission slit was set at 6 nm.

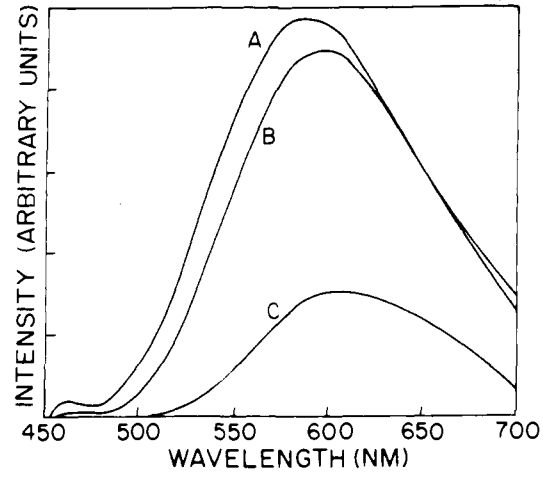

Figure 5. Uncorrected emission spectra of $[Cu(phen)(PPh_3)_2]^+$ at different exciting wavelengths: (A) 380 nm; (B) 400 nm; (C) 425 nm. The excitation slit was set at 7 nm, and the emission slit was set at 6 nm.

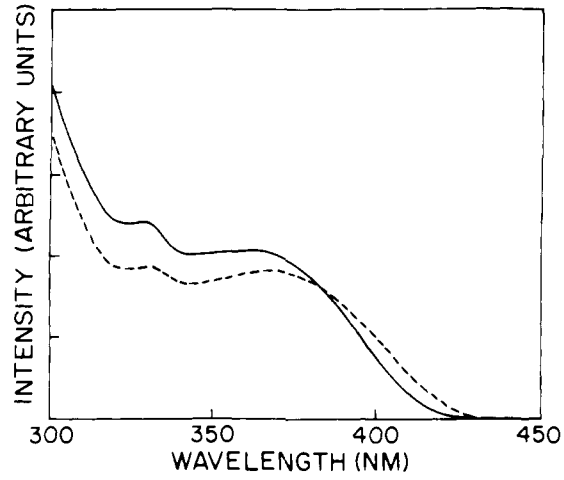

Figure 6. Corrected excitation spectra of $[Cu(5\text{-Cl-phen})(PPh_3)_2]^+$ at 77 K. The spectrum was monitored at 475 nm (—) and at 600 nm (---). The excitation slit was set at 6 nm, and the emission slit was set at 10 nm.

Table III. Luminescence Data at 77 K in 4:1 EtOH/MeOH

X	^{3}IL emission λ_{max},[b] nm	τ, ms	ϕ[c]	^{3}CT emission[a] λ_{max},[b] nm	τ, μs	ϕ[c]
		[Cu(5-X-phen)(PPh$_3$)$_2$]$^+$				
H	461	8.5 (1550[e])	1	600	103	1
	497				64[d]	
	528					
CH_3	473	10.5 (1650[e])	1.5	588	85	0.9
	504				61[d]	
	536					
Cl	483	14.5 (320[e])	2.1	590	75	0.6
	514				46[d]	
	550					
Ph	506 (sh)	34.5 (1050[e])	11.0	599	71	<0.1
	560				64[d]	
		[Cu(4,7-X$_2$-phen)(PPh$_3$)$_2$]$^+$				
H	461	8.5	1	600	103	1
	497					
	528					
Cl	490	12	2.0	601	85	0.7
	597					
CH_3	479	19	13	593	110	1.4
	513					
	579					
Ph	498	7.7	64	593	250	1.6
	537					
	568					

[a] Excitation wavelength is 385 nm except as noted. [b] Emission maxima are from corrected spectra. [c] Yields are relative to the 1,10-phenanthroline complex in each series. [d] Excitation wavelength is 425 nm. [e] Lifetime of free 5-X-phen ligand.

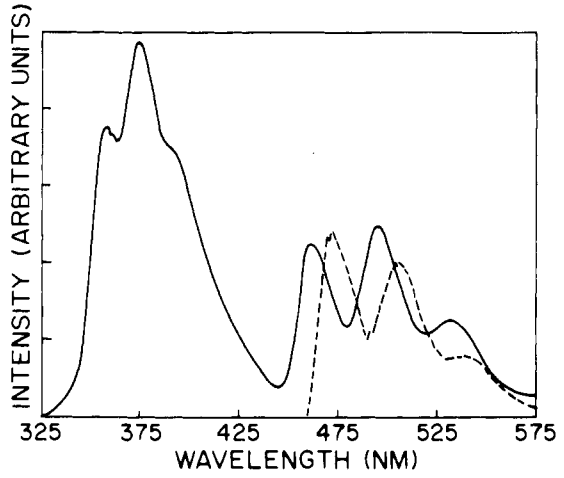

Figure 7. Uncorrected ^{3}IL emission of 4,7-Me$_2$-phen at 77 K: (—) free ligand excited at 300 nm; (---) [Cu(4,7-Me$_2$-phen)(PPh$_3$)$_2$]$^+$ excited at 380 nm and observed through the phosphoroscope. All slits were set at 8 nm except the excitation slit was set at 20 nm when the phosphoroscope was used.

The relative intensities of the ^{3}IL and ^{3}CT emissions also depend on the wavelength of excitation (Figure 5). Corrected excitation spectra of [Cu(5-Cl-phen)(PPh$_3$)$_2$]$^+$, presented in Figure 6, illustrate the same effect and extend farther toward the red when the ^{3}CT emission is monitored.

Time-Resolved Studies. The shorter lived ^{3}CT component is suppressed when the emission is viewed through a phosphoroscope. For example, Figure 7 contains the emission spectrum of [Cu(4,7-Me$_2$-phen)(PPh$_3$)$_2$]$^+$ when it is observed through a rotating-can phosphoroscope at 77 K. For comparison, the total emission (without phosphoroscope) of the free 4,7-Me$_2$-phen ligand is also presented. The similarities between the two spectra permit us to assign the complex's structured emission to the $^3\pi$–π^* state of the coordinated phenanthroline ligand, and the same assignment pertains to the structured emission of the other mixed-ligand complexes. While the IL emission spectra of the free and complexed ligands are similar, significant differences are apparent. (1) The IL fluorescence is quenched in the complex. Thus, the

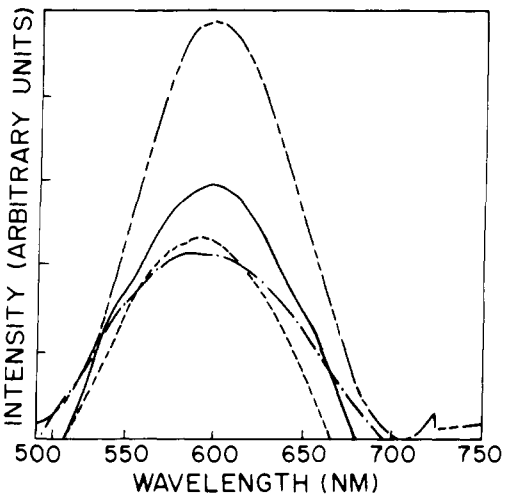

Figure 8. Time-resolved ^{3}CT luminescence spectra of [Cu(5-X-phen)(PPh$_3$)$_2$]$^+$ systems at 77 K: X = H (—); X = CH_3 (---); X = Cl (---); X = Ph (----). The gate was set at 5 ns and the spectra were taken 1 μs after the laser pulse. Relative intensities are not to scale.

^{1}IL emission of 4,7-Me$_2$-phen is visible at 400 nm in Figure 7, but it is absent in the total emission spectrum of [Cu(4,7-Me$_2$-phen)(PPh$_3$)$_2$]$^+$. (2) The vibronic band maxima of the ^{3}IL emission are red-shifted upon coordination. (3) Finally, the emission lifetime is decreased in the case of the complexed ligand (Table III).

In contrast, when pulsed laser excitation is used and the emission is sampled with the boxcar averager, the relatively long-lived ^{3}IL component is suppressed, and the ^{3}CT emission spectrum is detected. Time-resolved spectra of the ^{3}CT emissions from the [Cu(5-X-phen)(PPh$_3$)$_2$]$^+$ series are presented in Figure 8; luminescence data are compiled in Table III.

Discussion

Band Assignments. a. Charge-Transfer Absorption. The broad, structureless absorption bands of the [Cu(NN)(PPh$_3$)$_2$]$^+$ systems can be assigned as charge-transfer transitions because they do not occur in the spectra of [Cu(PPh$_3$)$_n$]$^+$ complexes or in the spectra of uncoordinated 1,10-phenanthroline derivatives. Moreover, analogous metal-to-ligand CT transitions are well-known in the visible spectra of [Cu(phen)$_2$]$^+$ and related systems.[4,34,35] In line with this reasoning,[35] the molar absorptivity of [Cu(phen)(PPh$_3$)$_2$]$^+$ at the CT maximum is about one-half as great as the corresponding absorptivity of [Cu(phen)$_2$]$^+$. Crosby and co-workers have proposed an alternative assignment of phosphine-to-phenanthroline interligand charge transfer.[36] However, this assignment can be discounted because corresponding absorption is not observed for [Ag(phen)(PPh$_3$)$_2$]$^+$.[33]

A qualitative energy-level diagram based on the calculations by Ito et al.[37] and by Daul et al.[38] is presented in Figure 9 for [Cu(phen)(PPh$_3$)$_2$]$^+$. Idealized C_{2v} symmetry has been assumed. The 1,10-phenanthroline ligand contains two low-lying π-antibonding orbitals which can act as acceptors during the CT process. Orgel has labeled them as ψ (antisymmetric) and χ (symmetric) according to their symmetry with respect to the C_2 axis which passes through the ligand.[39] Day and Sanders have pointed out that the CT absorption intensity derives in the main from the transitions which are polarized along the C_2 axis of the complex;[34] there are two such transitions indicated by arrows in Figure 9. The broad-band emission is analogous to the CT absorption and can be assigned to a ^{3}CT excited state.[23,25] Here the singlet–triplet

(34) Day, P.; Sanders, N. *J. Chem. Soc. A* **1967**, 1530–1536, 1536–1541.
(35) Phifer, C. C.; McMillin, D. R. *Inorg. Chem.* **1986**, *25*, 1329–1333.
(36) Crosby, G. A.; Highland, R. G.; Truesdell, K. A. *Coord. Chem. Rev.* **1985**, *64*, 41–52.
(37) Ito, T.; Tanaka, N.; Hanazaki, I.; Nagakura, S. *Bull. Chem. Soc. Jpn.* **1969**, *42*, 702–709.
(38) Daul, C.; Schlapfer, C. W.; Goursot, A.; Penigault, E.; Weber, J. *Chem. Phys. Lett.* **1981**, *78*, 304–310.
(39) Orgel, L. E. *J. Chem. Soc.* **1961**, 3683–3686.

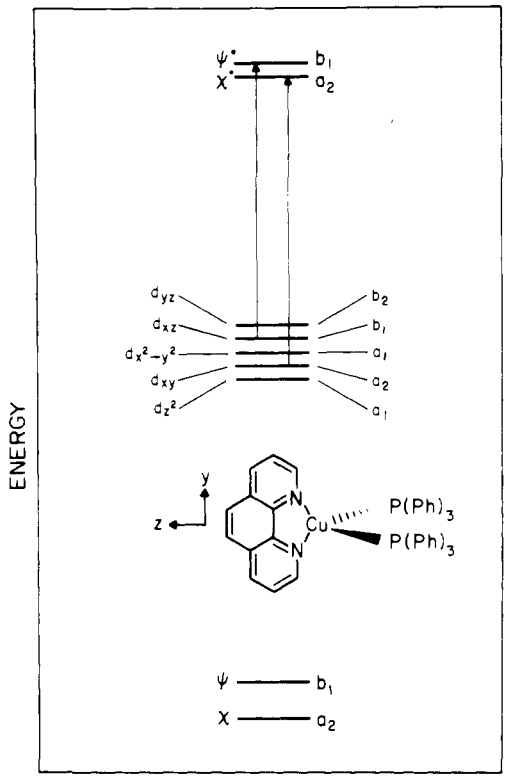

Figure 9. Energy level diagram and axis system for [Cu(phen)(PPh_3)$_2$]$^+$. The symmetry is C_{2v}, and the arrows indicate the z-polarized CT transitions. Labels ψ and χ designate molecular orbitals composed primarily of ligand-based π orbitals which are antisymmetric and symmetric, respectively, with respect to rotation about the twofold axis. Asterisks denote empty orbitals.

splitting is not large, and geometry differences between the ground state and the emitting CT state are more important factors determining the Stokes shift.

b. Intraligand Transitions. The vibronically structured absorbance which appears on the high-energy side of the CT absorption has been assigned to a $^1A_1$ state.[40] The relative energies of the ^{1}CT and $^1A_1$ (or ^{1}IL) transitions are not obvious from the one-electron energy-level diagram in Figure 9 because configuration interaction plays an important role in determining the energy of the IL excitation.[41] The vibronically structured component of the emission can be assigned to the corresponding $^3A_1$ (or ^{3}IL) state, where the Stokes shift reflects the singlet–triplet splitting.

Factors Responsible for Multiple Emissions. Systems which exhibit multiple emissions from thermally nonequilibrated excited states can be grouped into three different classes. The first consists of systems in which the sample is intrinsically heterogeneous, and this class includes the trivial case where impurity emissions are present. The second class is composed of systems in which heterogeneity is imposed by the environment. In the third, and most interesting, class the sample can be viewed as an essentially homogeneous system. In this case separate emissions arise because interconversion between distinct excited states is slow with respect to the competing decay processes.

a. Intrinsic Heterogeneity of the Sample. Sample heterogeneity may arise in several ways.[25] In our studies, ligand redistribution equilibria could cause problems because copper(I) complexes are labile. Previously, we have shown that extensive ligand redistribution can occur in the mixed-ligand systems when the phenanthroline ligand carries bulky substituents in the 2,9 positions.[30] However, if hydrogen atoms are present in the 2,9 positions (as is the case for all molecules relevant to this investigation), even in acetonitrile, only the following equilibrium is significant:[30]

$$[Cu(phen)(PPh_3)_2]^+ + CH_3CN \rightleftharpoons [Cu(phen)(PPh_3)(NCCH_3)]^+ + PPh_3 \quad (1)$$

The coordination of acetonitrile, an excellent ligand for the cuprous ion,[42] provides part of the driving force for eq 1 since the dissociation of PPh_3 is less significant in alcoholic media. In any case, as excess PPh_3 had no effect on the low-temperature emission spectra, eq 1 can be ignored for the present analysis.

Other potential sources of spurious emission can also be ruled out. First, the emission from the solvent blank is spectrally distinct and requires higher energy excitation. Although the samples slowly oxidize in solution under air, the decomposition requires days under room light. All of the measurements reported herein were made with freshly prepared samples.

b. Influence of Microenvironmental Effects. When the energy of an excited state is sensitive to the microenvironment and when energy transfer as well as solvent reorientation is slow, multiple emissions may be observed because discrete environments produce spectrally distinct emissions.[3,43] The hallmark of this phenomenon is a luminescence spectrum that varies with the excitation wavelength. The presence of microenvironmental heterogeneity is apparent from the spectral data in Figures 5 and 6 as well as the lifetime data in Table III. This is not surprising because formation of the CT excited state involves a strongly directional charge reorganization; hence the energy of the ^{3}CT emission should be sensitive to the solvent environment.[44,45]

However, our systems exhibit thermally nonequilibrated emissions from distinct electronic configurations. Moreover, evidence to be discussed below suggests that some interconversion between the two excited states—almost certainly an intramolecular process—occurs, albeit slowly. *This requires that the same molecule be capable of emitting from two different excited states.* Hence, our systems fall into class three described above. In the following discussion, in order to minimize effects associated with microenvironmental heterogeneity, we concern ourselves with a particular ensemble of molecules in solution—namely, those which are excited upon irradiation at the CT absorption maximum.

c. Nonequilibrating Excited States. The key to understanding the emission behavior of the [Cu(NN)(PPh_3)$_2$]$^+$ systems is recognition of the fact that the ^{3}IL and ^{3}CT states have different equilibrium geometries and that their interconversion can be inhibited at low temperatures in a rigid matrix. In particular, the equilibrium arrangement of the donor groups about the metal center is expected to be different in the two excited states. This follows because the ^{3}CT state formally involves a divalent copper center, and copper(II) complexes are subject to tetragonal distortions due to the Jahn–Teller effect.[46,47]

Vibronic interactions can also couple the ^{3}CT and ^{3}IL states. Figure 10 shows schematically how the two excited state surfaces might interact along a generalized nuclear displacement coordinate Q. This coordinate represents the positions of all nuclei in the system, including solvent, as the system traverses the minimum energy path between the two equilibrium geometries. The horizontal separation between the two minima in Figure 10 is a measure of the difference in the excited-state geometries. If this separation is large, the vibronic interaction is likely to have little influence on the equilibrium structures. This appears to be the case because the band shapes of the two components are essentially those of the corresponding unperturbed excited states.

Thus far, we have described how distinct emissions can arise from the same molecule with the familiar band shapes of the ^{3}CT

(40) Bray, R. F.; Ferguson, J.; Hawkins, C. J. *Aust. J. Chem.* **1969**, *22*, 2091–2103.
(41) Dewar, M. J. S.; Longuet-Higgins, H. C. *Proc. Phys. Soc., London, Sect. A* **1954**, *67*, 795–804.
(42) Macleod, I. D.; Muir, D. M.; Parker, A. J.; Singh, P. *Aust. J. Chem.* **1977**, *30*, 1423–1437.
(43) Weber, G.; Shinitsky, M. *Proc. Natl. Acad. Sci. U.S.A.* **1970**, *65*, 823–830.
(44) Saito, H.; Fujita, J.; Saito, K. *Bull. Chem. Soc. Jpn.* **1968**, *41*, 863–874.
(45) Demas, J. N.; Turner, T. F.; Crosby, G. A. *Inorg. Chem.* **1969**, *8*, 674–675.
(46) Pearson, R. G. *Symmetry Rules for Chemical Reactions*; Wiley-Interscience: New York, 1976; pp 12–19, 187–190.
(47) Burdett, J. K. *Molecular Shapes*; Wiley-Interscience: New York, 1980; pp 172–185.

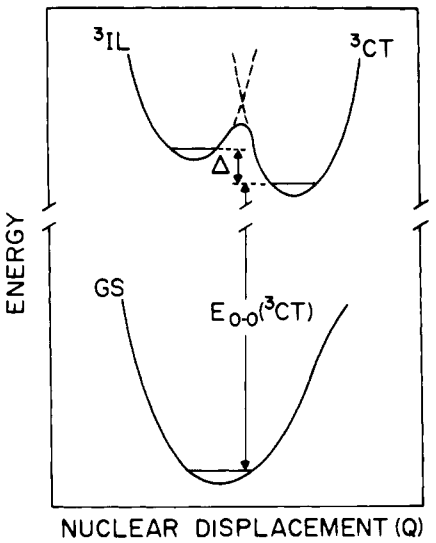

Figure 10. Potential energy surfaces for the ground state and the lowest energy excited state of a $[Cu(NN)(PPh_3)_2]^+$ system. The dashed lines indicate the zero-order ^{3}IL and ^{3}CT surfaces. The zero-zero energy of the ^{3}CT state and the difference between the zero-zero energies of the ^{3}CT and ^{3}IL states are also indicated. A vibronic interaction occurs between the dashed surfaces along the nuclear displacement coordinate Q.

Table IV. Zero-Zero Energies[a]

X	$E_{0-0}(^3CT)$,[b,c] cm^{-1}	$E_{0-0}(^3IL)$,[c] cm^{-1}	Δ,[d] cm^{-1}
	$[Cu(5\text{-X-Phen})(PPh_3)_2]^+$		
H	21 000	21 600	600
CH_3	20 800	21 200	400
Cl	20 700	20 700	0
Ph	20 800	19 800	-1000
	$[Cu(4,7\text{-X}_2\text{-phen})(PPh_3)_2]^+$		
H	21 000	21 600	600
Cl	20 400	20 600	200
CH_3	21 400	21 100	-300
Ph	20 800	20 200	-600

[a] Excitation at 385 nm. [b] Calculated from eq 2. [c] Emission energies from corrected spectra plotted vs. energy. [d] $\Delta = E_{0-0}(^3IL) - E_{0-0}(^3CT)$.

and ^{3}IL excited states. The emission intensities remain to be considered, but first we must establish the relative energies of the excited states.

Energies of the Vibrationally Relaxed Excited States. The zero-zero energy, i.e., the energy difference between the lowest vibrational levels of the ground and excited states, is the proper measure of the energy of an excited state and is most easily determined from a plot of the emission spectrum vs. energy. To convert from a wavelength representation to an energy representation, the emission intensity at each wavelength must be multiplied by the wavelength squared in order to account for the energy dependence of the band-pass function.[48] The zero-zero energy of the ^{3}IL state can be read directly from the spectrum as it corresponds to the energy of the highest energy vibronic component of the emission.[49] These values are compiled in Table IV. Not surprisingly, the ^{3}IL energies are sensitive to substitution at either the 5 or the 4,7 positions.

Since there is no resolved vibronic structure on the ^{3}CT emission, an alternate method of estimating the zero-zero energy must be used. In view of the fact that the Franck-Condon states reached during the absorption and the emission processes involve significant vibrational excitation, the average of the energy maxima provides a reasonable estimate of the zero-zero energy. Since absorption occurs to the ^{1}CT state, which occurs about 1000 cm^{-1} above the ^{3}CT state,[10] eq 2 was used to calculate the zero-zero energies of the respective ^{3}CT excited states:

$$E_{0-0}(^3CT) = \tfrac{1}{2}[E^{abs}_{max} - 1000) + E^{em}_{max}] \quad (2)$$

where E^{abs}_{max} and E^{em}_{max} are the maxima observed in the absorption and emission spectra plotted against energy in cm^{-1}. These results are also listed in Table IV. In arriving at eq 2, we have ignored the possibility that more than one CT state is present for each multiplicity. In view of the complexity of the energy scheme in Figure 9, this may be an oversimplification. If more than one state is involved, the maxima in the experimental spectra relate to absorption and emission envelopes, as opposed to individual absorption and emission transitions. For this reason comparisons are based on *trends* in the calculated zero-zero energies.

Parenthetically, we may note that the zero-zero energy of the ^{3}CT excited state is sensitive to substitution at the 4,7 positions but relatively insensitive to substitution at the 5 position. This might be explained by the fact that the $2p_x$ orbital of the C5 carbon makes a minor contribution to the ψ^* orbital of phen, whereas the $2p_x$ orbitals of the C4 and C7 carbons carry relatively large coefficients in the ψ^* and χ^* orbitals.[37]

Importance of the Energy Separation between the ^{3}CT and ^{3}IL States. The evidence presented below suggests that the energy gap influences the excited-state dynamics of the $[Cu(NN)(PPh_3)_2]^+$ systems in two ways. On the one hand, the energy gap determines the extent of configuration interaction; hence it affects the intrinsic rates with which the excited states decay to the ground state. In addition, the energy gap affects the rates of interconversion between the two excited states.

a. Effect of Configurational Mixing. Variations in the degree of configurational mixing may help explain the dependence of the ^{3}CT emission lifetime on the exciting wavelength (Table III). For the 5-X-phen derivatives, the lifetime of the ^{3}CT state decreases noticeably when the excitation wavelength increases, except for the 5-Ph-phen complex. When long-wavelength excitation is used, molecules with lower energy ^{3}CT states are excited (Figure 5), and the energy gap between the ^{3}IL and ^{3}CT excited states is, in effect, enlarged. If this results in less ^{3}IL character in the ^{3}CT state, a decrease in the ^{3}CT lifetime is to be expected. The fact that the lifetime of the 5-Ph-phen complex is less sensitive to the exciting wavelength may be telling because it is the only member of the series in which the ^{3}IL state falls below the ^{3}CT state.

On the other hand, the decrease in the lifetime might simply be explained by the energy gap law as the separation between the ^{3}CT state and the ground state is also decreased. Better evidence for the importance of configurational mixing comes from comparisons with related silver systems. Complexation to silver or copper decreases the lifetime of the ^{3}IL state because of a heavy atom effect. Yet, despite the fact that silver is a heavier metal than copper, the lifetime of the ^{3}IL state of $[Ag(phen)_2]^+$ (85 ms at 77 K[50]) is substantially longer than the ^{3}IL lifetime of any of the $[Cu(NN)(PPh_3)_2]^+$ systems. This is presumably explained by the fact that the ^{3}CT states occur at higher energies in the silver systems.

b. Internal Conversion. Direct evidence of conversion between the ^{3}IL and ^{3}CT excited states is lacking, but this process would explain trends in the lifetimes and emission quantum yields of the 5-X-phen series. The most striking trend is that the ^{3}IL excited state lifetime varies *inversely* with its zero-zero energy, contrary to the well-known energy gap law. However, this trend is easily explained if internal conversion to the ^{3}CT state provides a means of depopulating the vibrationally relaxed ^{3}IL excited state.

At least in a formal sense, conversion from the ^{3}IL state to the ^{3}CT state can be regarded as an intramolecular electron-transfer process involving the exchange of an electron between a metal 3d orbital and a π-bonding orbital of the ligand.[25] As such, the conversion rate can be analyzed in terms of Marcus theory.[51] Indeed, the double minimum potential energy surface in Figure 10 has the classic shape of a reaction surface in the Marcus

(48) Lakowicz, J. R. *Principles of Fluorescence Spectroscopy*; Plenum Press: New York, 1983; pp 42, 43.
(49) Herkstroeter, W. G.; Lamola, A. A.; Hammond, G. S. *J. Am. Chem. Soc.* **1964**, *86*, 4537-4540.
(50) Tamilarasan, R.; McMillin, D. R., unpublished results.
(51) Marcus, R. A.; Sutin, N. *Biochim. Biophys. Acta* **1985**, *811*, 265-322.

Formulation,[51,52] The full theory deals with numerous factors including reorganization energies of the solvent and the reactants. For our systems most of these effects are likely to be constant; the key factor which varies is the driving force which we take to be Δ, the difference between the zero–zero energies of the two excited states. Theory predicts that the rate of electron transfer inherently has a parabolic dependence on the driving force. However, for small Δ (the regime of interest here) the rate is expected to increase with the driving force.[51,53] Consistent with the theoretical prediction, the data in Tables III and IV show that the lifetime of the ^{3}IL state decreases as the driving force for conversion to the ^{3}CT state becomes more favorable. It is tempting to extend this argument in order to rationalize the details of the emission quantum yields. Thus, the ^{3}CT emission yield increases as the ^{3}IL lifetime decreases, and the ^{3}IL emission yield is highest for the 5-Ph-phen system where invernal conversion from the ^{3}CT state is feasible. However, many other processes influence the emission yields (vide infra).

In contrast, the lifetimes and emission yield of the 4,7-X_2-phen complexes do not correlate well with the Δ values. The one exception is the ^{3}IL emission yield which increases monotonically as Δ ranges more negative. However, the ^{3}CT emission yields are virtually independent of Δ, and the emission lifetimes show no consistent trends. Here the influence of the internal conversion process may be obscured by competing kinetic effects. Previous studies have shown that substituents in the 4,7 positions have a pronounced effect on the radiative and nonradiative rates of phenanthroline complexes,[54,55]

Energy Flow Prior to Emission. If conditions are favorable, it should be possible to observe the internal conversion process by time-resolved techniques.[56,57] For example, if the ^{3}IL state of [Cu(5-Ph-phen)(PPh_3)$_2$]$^+$ were populated strictly by internal conversion from the vibrationally relaxed ^{3}CT excited state, the time constant for the *rise* of the ^{3}IL emission should be equal to the lifetime of the ^{3}CT emission. Similarly, if the ^{3}IL state of [Cu(phen)(PPh_3)$_2$]$^+$ converts to the ^{3}CT state on a millisecond time scale, the ^{3}CT emission should exhibit a delayed component with a lifetime of the order of milliseconds. Although we looked for evidence of a slow rise time in the oscilloscope traces, we were unable find one with the available equipment. However, even a negative result would not necessarily be inconsistent with model. The problem is that internal conversion from a neighboring, vibrationally relaxed excited state is only one of a number of competing pathways which affect population of a given emitting state. Neither the ^{3}IL nor the ^{3}CT state is populated directly; the major absorbance at the excitation wavelength can be attributed to one or more ^{1}CT excited states, although the ^{1}IL absorption tails into this region as well. Once excited, any of these states could convert into the ^{3}IL or the ^{3}CT excited state. Hence, a whole network of branching processes may precede formation of the vibrationally relaxed ^{3}CT and ^{3}IL excited states. If these processes are efficient, internal conversion from the neighboring, vibrationally relaxed triplet state may make a negligible contribution to the population of a given emitting state.

Conclusions

Thermally nonequilibrated emissions from ^{3}CT and ^{3}IL excited states have been characterized for a series of systems of the type [Cu(NN)(PPh_3)$_2$]$^+$ where NN denotes a 5-X-phen or 4,7-X_2-phen derivative. The ^{3}CT emission is broad and unstructured with an emission lifetime of the order of 100 μs, while the ^{3}IL emission exhibits vibronic structure and has a lifetime of the order of 10 ms. As the energy separation between the ^{3}CT and ^{3}IL excited states varies, the relative intensities of the two emission components change in a predictable manner. The emission intensity is always smaller for the higher energy excited state, and when the separation is as large as 1000 cm^{-1}, the emission from the higher energy component has nearly vanished. Although microenvironmental heterogeneity is present, we conclude that multiple emissions occur because interconversion between the ^{3}IL and ^{3}CT states is inhibited in a low-temperature, rigid matrix owing to the fact that the vibrationally relaxed excited states have different molecular geometries. Although the data might be equally well explained in terms of nested excited state surfaces, this seems unlikely in view of the differences in the formal oxidation state of the metal center in the ^{3}IL and ^{3}CT excited states. The ^{3}IL emission lifetimes of the 5-X-phen derivatives can be understood in terms of a radiationless process connecting the ^{3}IL and ^{3}CT excited states. This conversion has been interpreted as an intramolecular electron-transfer process with a rate that depends upon the driving force. However, this process has not been detected in time-resolved emission studies, and it may be of minor significance in the determination of emission yields.

Acknowledgment. This work was supported by the National Science Foundation through Grant No. CHE-8414267. The authors wish to thank Cynthia E, A. Palmer for assisting with the lifetime measurements.

(52) Guarr, T.; McLendon, G. *Coord. Chem. Rev.* **1985**, *68*, 1–52.
(53) Miller, J. R.; Calcaterra, L. T.; Closs, G. L. *J. Am. Chem. Soc.* **1984**, *106*, 3047–3049.
(54) Crosby, G. A.; Watts, R. J. *J. Am. Chem. Soc.* **1972**, *94*, 2606–2614.
(55) Lin, C. T.; Bottcher, M.; Chou, M.; Creutz, C.; Sutin, N. *J. Am. Chem. Soc.* **1976**, *98*, 6536–6544.
(56) DiBartolo, B. *Optical Interactions in Solids*; Wiley: New York, 1968; pp 442–446.
(57) Balzani, V.; Moggi, L.; Manfrin, M. F.; Bolletta, F.; Laurence, G. S. *Coord. Chem. Rev.* **1975**, *15*, 321–433.